Poly(ethylene oxide) Macromonomers. 7. Micellar Polymerization in Water

Koichi Ito,* Kazuo Tanaka, Hiroshige Tanaka, Genji Imai, Seigou Kawaguchi, and Shinichi Itsuno

Department of Materials Science, Toyohashi University of Technology, Tempaku-cho, Toyohashi 441, Japan

Received July 27, 1990; Revised Manuscript Received October 19, 1990

ABSTRACT: Poly(ethylene oxide) (PEO) macromonomers (1 and 2) carrying a methyl, *n*-butyl, *tert*-butyl, *n*-octyl, or *n*-octadecyl group as the ω-end and a *p*-vinylbenzyl or methacryloyl group as the α-end were prepared, and their radical polymerizations in water were found to occur unusually rapidly as a result of their organization into micelles. The micelle sizes were estimated with the nonpolymerizable macromonomer models (3 and 4) by laser light scattering measurements. Significant effects of ω-alkyl groups and the PEO chain lengths on the polymerizability were observed and found to parallel the molecular density of the corresponding model, measured by the degree of aggregation (m) divided by the micelle volume (V_m). The hydrophobic α-ends as polymerizing groups are very likely to be concentrated and organized in the micelle core, with the hydrophilic PEO chains coiling in the surrounding shell, allowing a very rapid polymerization to an amphiphilic comb polymer of a very high molecular weight.

Introduction

A number of macromonomers have so far been developed to be useful for designing a vast variety of well-defined graft copolymers.[1] Along with extensive studies on their preparation and practical applications, there has been considerable progress in understanding the macromonomer's behavior in copolymerization with a conventional, trunk-forming comonomer, which is of fundamental importance in determining the primary structure of the resulting graft copolymers. Among others, Tsukahara[2] and Gnanou[3] and their co-workers have shown clearly with polystyrene macromonomers that their reactivities are essentially determined by the chemical nature of their terminal copolymerizing groups, so long as they are thermodynamically compatible with, or at least able to interpenetrate without difficulty, the trunk polymer chains, i.e., the polymer radicals from the comonomers employed. The so-called kinetic excluded-volume effect, if any, appears to be negligibly small. Therefore, an apparent decrease in the macromonomers's reactivity compared to that of the low molecular weight analogue, as often observed in such cases including poly(ethylene oxide) (PEO),[4] polyisobutylene,[5] and poly(dimethylsiloxane),[6,7] could be reasonably ascribed to thermodynamic repulsion or incompatibility between the macromonomer and the trunk polymer from the comonomer, resulting in phase separation in extreme cases. Monomer partition at the polymerization site, which may differ in the composition from the bulk, can also be a factor for changing the apparent reactivity in the cases including a selective solvent[8] or in a dispersion polymerization system.[9]

On the other hand, homopolymerization of macromonomers to afford comb- or starlike polymers has recently been of considerable concern in view of a very specific kinetic behavior. In particular, the termination rate constants in the radical polymerization of polystyrene[10,11] and syndiotactic poly(methyl methacrylate) macromonomers[12] have been estimated to be even 3–5 orders of magnitude smaller than those of the low molecular weight monomers, probably due to their highly crowded, multibranched segments in their diffusion-controlled polymer–polymer reactions.

The present paper aims to summarize and discuss our results[13] of radical polymerization of PEO macromonomers (1 and 2), which have been our interest because of their amphiphilic property of being soluble in such a wide range of solvents as benzene and water. Their polymerization in water was indeed found to occur unusually rapidly, probably as a result of their organization into micellar aggregates. This appears to be a feature general for

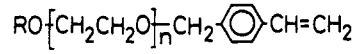

(1) R-PEO-VB-n

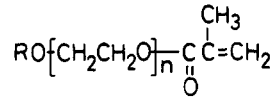

(2) R-PEO-MA-n

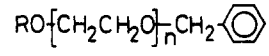

(3) R-PEO-Bz-n

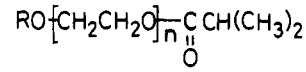

(4) R-PEO-IB-n

R= CH_3 (C_1), nC_4H_9 (C_4), $C(CH_3)_3$ (tC_4)
nC_8H_{17} (C_8), $nC_{18}H_{37}$ (C_{18})

amphiphilic macromonomers, and their organized polymerizations will be promising to realize fixation of the amphiphilic microdomains. The macromonomers 1 and 2 will be abbreviated hereafter by R-PEO-VB-*n* and R-PEO-MA-*n*, respectively, to specify the ω-alkyl group by R; C_1 for methyl, C_4 for *n*-butyl, tC_4 for *tert*-butyl, C_8 for *n*-octyl, and C_{18} for *n*-octadecyl. The number-average degree of polymerization of the PEO chain is specified by the number for n, while VB and MA stand for the α-end groups, *p*-vinylbenzyl and methacryloyl, respectively. Their nonpolymerizable models, 3 (R-PEO-Bz-*n*) and 4 (R-PEO-IB-*n*), served for light scattering measurements to estimate the micelle size.

0024-9297/91/2224-2348$02.50/0

Table I
Characterization of Macromonomers and Their Nonpolymerizable Models[a]

abbrev	ω-group R[a]	α-group X[a]	n^a NMR[b]	n^a GPC[c]	M_w/M_n GPC[c]
C_1-PEO-VB-17	methyl	*p*-vinylbenzyl	17	15	1.25
C_1-PEO-VB-25	methyl	*p*-vinylbenzyl	25	26	1.26
C_1-PEO-VB-45	methyl	*p*-vinylbenzyl	45	43	1.19
C_1-PEO-VB-60	methyl	*p*-vinylbenzyl	60	59	1.10
C_1-PEO-MA-25	methyl	methacryloyl	25	27	1.16
C_4-PEO-VB-39	*n*-butyl	*p*-vinylbenzyl	39	40	1.14
tC_4-PEO-VB-24	*tert*-butyl	*p*-vinylbenzyl	24	24	1.08
tC_4-PEO-VB-32	*tert*-butyl	*p*-vinylbenzyl	32	30	1.09
tC_4-PEO-MA-24	*tert*-butyl	methacryloyl	24	24	1.08
C_8-PEO-VB-43	*n*-octyl	*p*-vinylbenzyl	43	42	1.16
C_{18}-PEO-VB-35	*n*-octadecyl	*p*-vinylbenzyl	35	36	1.04
C_1-PEO-Bz-25	methyl	benzyl	25	27	1.16
C_1-PEO-Bz-45	methyl	benzyl	45	43	1.18
C_1-PEO-IB-25	methyl	isobutyroyl	25	27	1.16
C_4-PEO-Bz-39	*n*-butyl	benzyl	39	40	1.08
tC_4-PEO-Bz-32	*tert*-butyl	benzyl	32	30	1.07
C_8-PEO-Bz-43	*n*-octyl	benzyl	43	42	1.03
C_{18}-PEO-Bz-35	*n*-octadecyl	benzyl	35	36	1.08

[a] $RO-(CH_2CH_2O)_n-X$. [b] Determined by ^1H NMR from the ratio of peak areas of oxyethylene to benzylmethylene protons. [c] Determined by GPC calibrated with PEO standard samples.

Experimental Section

Materials. Monomers, solvents, α,α′-azobis(isobutyronitrile) (AIBN), *p*-vinylbenzyl chloride (VBC), and methacryloyl chloride (MAC) were purified as described before.[4] Potassium *tert*-butoxide and 2-methoxyethoxide were prepared under vacuum as before.[4] Potassium *n*-butoxide was prepared under vacuum by the reaction of potassium mirror with excess *n*-butanol, followed by evaporation of the excess alcohol, and finally dispersed in tetrahydrofuran (THF). Potassium *n*-octoxide was prepared similarly by reacting *n*-octanol solution in THF with excess potassium at about 55 °C for 3 h, when the evolution of the hydrogen gas was little observed, leaving a clean solution and excess potassium, which was filtered out by a glass filter. 4,4′-Azobis(4-cyanovaleric acid) (AVA) from Aldrich, deuterated solvents, $CDCl_3$, C_6D_6, and D_2O, from Aldrich or CEA, and sodium hydride from Kishida Chemicals were used as supplied.

Macromonomers. C_1, tC_4, C_8-PEO-VB, and C_1-PEO-MA were prepared under vacuum by living anionic polymerizations of ethylene oxide with the corresponding potassium alkoxides as the initiators, followed by end capping with VBC or MAC, according to the procedure described previously.[4] C_{18}-PEO-VB was prepared also under vacuum from monostearyl ether of poly(ethylene glycol), supplied from the Takemoto Oil & Fat Co., Ltd., by reacting with excess sodium hydride in benzene, to afford the alkoxide solution, which was filtered and reacted with excess VBC. All the macromonomers were purified similarly as described before[4] and examined by GPC and ^1H NMR to verify the structures. Sharp distribution in the molecular weights and the end functionality above 95% were satisfactorily confirmed in each case. The results of characterization were summarized in Table I, together with those of the nonpolymerizable macromonomer models, which were prepared similarly by end capping with benzyl chloride or isobutyroyl chloride in place of VBC or MAC. Low molecular weight oligomer monomers, such as C_1-PEO-VB-1, C_1-PEO-VB-4, and C_1-PEO-MA-3, were prepared from the corresponding mono- or oligo(ethylene glycol) monomethyl ether according to the procedure described before.[4] Only C_1-PEO-MA-3 was soluble in water among the oligomers studied.

Polymerization. Macromonomers were polymerized at 60 °C either in benzene with AIBN or in water with AVA under argon atmosphere. Polymerization was generally monitored in the corresponding deuterated solvent by means of ^1H NMR by following the disappearance of the double-bond peaks in reference to the oxyethylene peaks, as exemplified in Figure 1. Conversions were calculated by the equation

$$\text{conversion}\ (\%) = [1 - (b/a)_t/(b/a)_0] \times 100 \qquad (1)$$

where $(b/a)_t$ and $(b/a)_0$ are the ratios of the peak area of the double-bond protons to that of the oxyethylene protons at a given time, t, and at $t = 0$, respectively. The polymerization in water was so rapid that it was monitored throughout in the NMR probe at 60 °C, while that in benzene was so slow that the NMR tube was placed in an oil bath of 60 °C except for the time of NMR measurements. Gel permeation chromatography (GPC) was also used to check the conversion of tC_4-PEO-VB. The polymerization mixture, after being freeze-dried, was subjected to a GPC measurement in THF to analyze the relative peak areas due to the macromonomer and its polymer, by assuming their same response to the refractive index (RI) detector. Polymerization of a model monomer, C_1-PEO-VB-1, in benzene was also checked by a conventional method of weighing after isolation of the polymer by precipitation into hexane. Some of the poly(macromonomer)s were isolated from the polymerization mixture by fractional precipitation from benzene–hexane mixture at 40 °C and confirmed by GPC for the removal of the unreacted macromonomers.

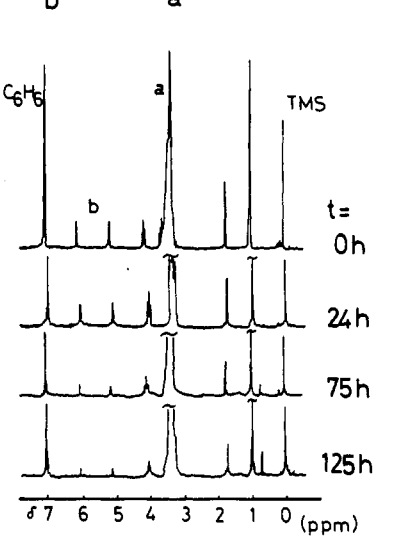

Figure 1. Monitoring by ^1H NMR of the polymerization of C_1-PEO-VB-24 in benzene.

Measurements. GPC was measured with a HPLC of Jasco (Japan Spectroscopic Co., Ltd., Hachioji, Tokyo 192), TRIROTAR-III, equipped with an RI detector, Shodex SE-11, and an appropriate combination of columns, Shodex A-801 to A-804 depending on the molecular weight range. THF was used as an eluent at a flow rate of 1 mL/min at 40 °C. Molecular weight was calibrated with standard samples of PEO from Tosoh Co., Ltd. ^1H NMR spectra were recorded on a JEOL JNM-GX 270 FT spectrometer in $CDCl_3$, in C_6D_6 with tetramethylsilane (TMS)

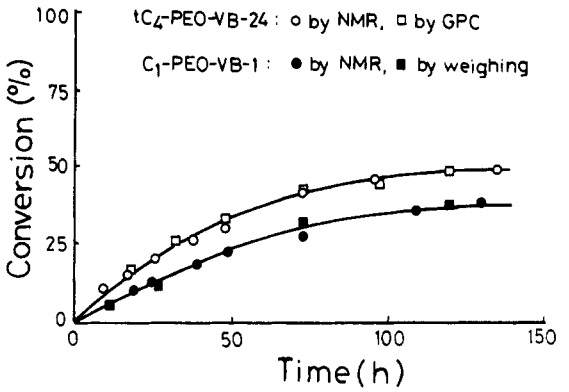

Figure 2. Conversion vs time plots for polymerization of tC_4-PEO-VB-24 (○ by NMR, □ by GPC) and C_1-PEO-VB-1 (● by NMR, ■ by weighing) in benzene with [M] = 45 mmol/L and [AIBN] = 2.25 mmol/L.

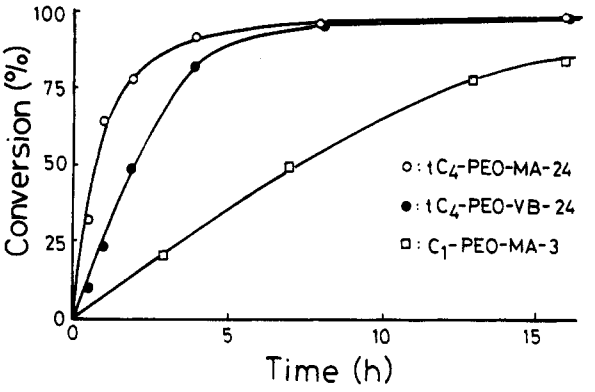

Figure 3. Conversion vs time plots for polymerization of tC_4-PEO-VB-24 (●), tC_4-PEO-MA-24 (○), and C_1-PEO-MA-3 (□) in water with [M] = 45 mmol/L and [AVA] = 0.45 mmol/L.

or hexamethyldisiloxane (HMDS), or in D_2O with sodium 2,2-dimethyl-2-silapentane-5-sulfonate (DSS) as an internal standard. Four to eight scans with a pulse delay time of 30–60 s were satisfactory to reproducible results for the structure and conversion analyses. Light scattering was measured at 25.0 °C with a photometer system, LS-601, Union Giken Co., Ltd., equipped with a He–Ne laser of 632.8 nm. The sample solution was filtered through a membrane of pore size 1 or 0.45 μm, Toyo Roshi Co., Ltd. The refractive index increment (dn/dc) was measured at 25.0 °C with a refractometer, RF-600 of the C. N. Wood Mfg. Co., Ltd., or RM-102 of the Ootsuka Electronics Co., Ltd.

Results and Discussion

General Polymerization Behavior of PEO Macromonomers. The copolymerization of the PEO macromonomers (M_1) with a conventional comonomer (M_2) such as styrene was studied in detail previously,[4] with the result that the M_1's relative reactivity, $1/r_2$, where r_2 is the monomer reactivity ratio of M_2, decreased with an increasing degree of polymerization of M_1. This means that the propagating polymer radical, which can be approximated as a poly-M_2 radical under the condition employed, reacts with greater difficulty with M_1 than with the lower molecular weight model monomers. A thermodynamic repulsive interaction between the unlike, imcompatible polymer chains, i.e., M_1 and poly-M_2, was proposed as a most important factor for decreasing their apparent reactivities.

In contrast, the homopolymerization of the macromonomer should not be affected by thermodynamic compatibility or incompatibility between the polymer radical and the macromonomer because of their same chemical constitution. In fact, the macromonomers were found to polymerize more rapidly both in benzene and in water than the low molecular weight model monomers, as shown in Figures 2 and 3. The estimation of conversions by means of ^1H NMR is in satisfactory agreement with that by GPC or by weighing. The higher polymerization rates of the macromonomers can be reasonably ascribed to a lower rate of diffusion-controlled termination due to their highly crowded segments, as will be discussed in more detail later.

Most important to be noted, however, is the fact that the polymerization in water, Figure 3, is surprisingly higher, in spite of the lower initiator concentration, than that in benzene, Figure 2. The former is almost quantitative after about 5 h, while the latter is very slow and levels off below 50% conversion after 4 days or so. Thus in benzene, the employed condition of very low concentrations of both the macromonomer and the initiator on the molar basis may well result in the "dead-end" phenomenon[14] as observed. In water, however, these amphiphilic macromonomers will aggregate to form micelles with their

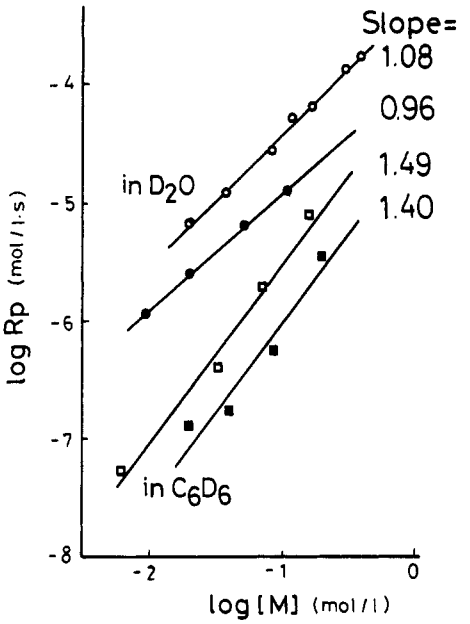

Figure 4. log–log plots of R_p vs [M] for polymerization of tC_4-PEO-VB-24 (● in water, ■ in benzene) and tC_4-PEO-MA-24 (○ in water, □ in benzene). [AVA] = 0.45 mmol/L in water, and [AIBN] = 9.9 mmol/L in benzene.

hydrophobic groups in the core and the hydrophilic PEO chains in the surrounding shell. This aggregation will locally concentrate and orientate the hydrophobic polymerizing groups to enhance their polymerization. This will be the subject that follows. The difference in the initiators, AVA in water and AIBN in benzene, cannot be a factor because the former decomposes more slowly than the latter,[15] contrary to the observed polymerization rates.

Kinetics of Polymerization. The rate of polymerization, R_p, of tC_4-PEO-VB and -MA was estimated from the initial slope of the conversion vs time plots, with the results given in Figures 4 and 5. It is clear in these log–log plots that R_p in water is 1 or 2 orders of magnitude higher than that in benzene. The exponent of the dependence of R_p on the concentrations of the monomer, [M], and the initiator, [I], indicates the following relationships to hold roughly within the concentration range studied

$$R_p \propto [M]^{1.5}[I]^{1/2} \quad \text{in benzene} \tag{2}$$

and

$$R_p \propto [M][I]^{1/2} \quad \text{in water} \tag{3}$$

The latter is in accordance with the conventional rela-

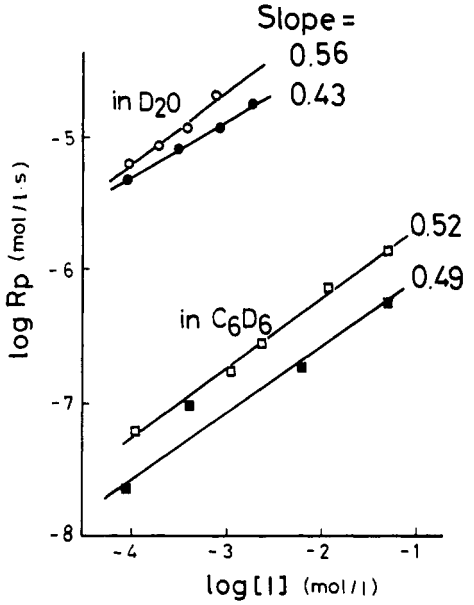

Figure 5. log–log plots of R_p vs [I] for polymerization of tC_4-PEO-VB-24 (● in water, ■ in benzene) and tC_4-PEO-MA-24 (○ in water, □ in benzene). [M] = 45 mmol/L.

tionship in radical polymerization[14] as

$$R_p = k_p(2fk_d/k_t)^{1/2}[M][I]^{1/2} \quad (4)$$

where k_p and k_t are the rate constants of propagation and termination, respectively, while k_d and f are the decomposition rate constant and the initiator efficiency of the initiator, respectively.

The square-root dependence of [I], as observed both in benzene and in water, clearly supports the conventional bimolecular termination of the polymer radicals to prevail also for the polymerization of the macromonomers, at least under the conditions employed. Since these radical termination reactions are now well-known to be diffusion-controlled,[14,16] they should be retarded by increasing viscosity of the medium, thus by restricting the segmental motion of the involved polymer radicals. This can be a reason for the higher rate of polymerization of the macromonomer as compared to the low molecular weight model monomer, as found in Figures 2 and 3. The dependence on [M] may become higher than the first order as observed in benzene, as a result of the inverse dependence of k_t on the medium viscosity, which increases with the monomer concentration, because the monomer here is itself a polymer of a reasonable molecular weight.[17] The results in Figure 4 or eq 2 are thus reasonable in reflecting this situation. Tsukahara and co-workers[10] reported an even much higher order of dependence on [M] for the methacrylate-ended polystyrene macromonomer of a molecular weight around 13 000 in benzene. Recent ESR studies[11] estimated the decrease in k_t by a factor of 10^3, together with the decrease in k_p by a factor of about 10, as compared to methyl methacrylate. A similar situation may also be true in our system in benzene.

In water, however, an apparently normal kinetic behavior, eq 3, was observed with an unusually high polymerization rate. This can be expected in the context of the micellar polymerization by considering that k_t may be extremely low and remains constant in the organized micellar environment, independent of the overall monomer concentration, which is much higher than the critical micelle concentration (cmc), as will be shown later. The linear dependence of R_p on [M] may simply reflect a linear dependence of the concentration of the micelles, which are the sites of polymerization, on the overall concentration. This situation may appear to be somewhat similar to that in the conventional emulsion polymerization[14] but it is different in that the monomers here are themselves the micelle-forming surfactants and that the system remains apparently clear throughout the polymerization. The same normal kinetics as in eq 3 has been reported by Yeoh and co-workers[18] for the polymerization of a surfactant monomer such as sodium 11-[*N*-(methacryl)amido]-undecanoate.

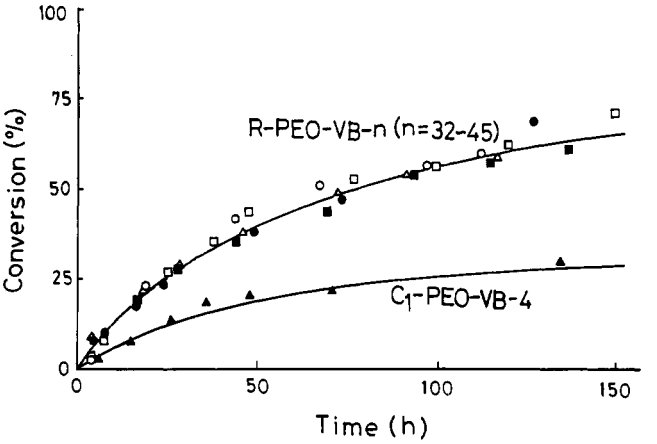

Figure 6. Conversion vs time plots for polymerization of C_1-PEO-VB-45 (●), C_4-PEO-VB-39 (■), tC_4-PEO-VB-32 (△), C_8-PEO-VB-43 (○), C_{18}-PEO-VB-35 (□), and C_1-PEO-VB-4 (▲) in benzene with [M] = 45 mmol/L and [AIBN] = 2.25 mmol/L.

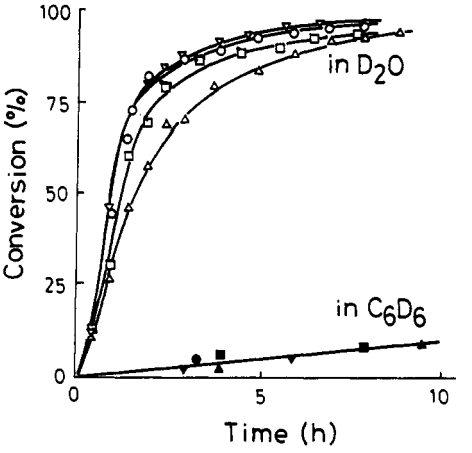

Figure 7. Conversion vs time plots for polymerization of C_1-PEO-VB-17 (▽), C_1-PEO-VB-25 (○), C_1-PEO-VB-45 (□), and C_1-PEO-VB-60 (△) in water with [M] = 45 mmol/L and [AVA] = 0.45 mmol/L. Solid symbols refer to the corresponding polymerization in benzene with [M] = 45 mmol/L and [AIBN] = 2.25 mmol/L.

Effects of ω- and α-Terminal Groups and of PEO Chain Lengths on the Polymerizability. Figure 6 shows that the ω-alkyl groups of the macromonomers, R-PEO-VB, have little effect on their polymerizability in benzene and that they polymerize more rapidly than the lower molecular weight homologue, C_1-PEO-VB-4. This result is in line with the previous discussions. Figure 7 shows that the chain lengths of PEO have little effect on the polymerization in benzene. These results indicate that the chemical reactivity of the terminal double-bond determining k_p and the mutual segmental diffusion of the polymer radicals determining k_t do not so significantly depend either on the ω-alkyl groups or on the PEO chain lengths, at least within the range studied, i.e., C_1 to C_{18} for R and 17–60 for n.

In water, however, significant effects are observed. From the results with R-PEO-VB-n in Figures 7 and 8, we can summarize the effects of R and n on R_p in the decreasing

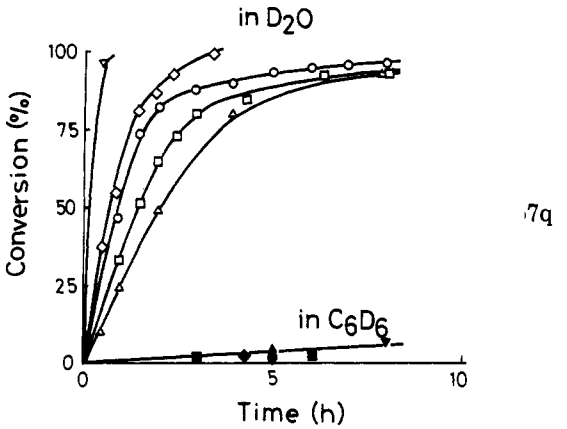

Figure 8. Conversion vs time plots for polymerization of C_1-PEO-VB-25 (○), C_4-PEO-VB-39 (□), tC_4-PEO-VB-32 (△), C_8-PEO-VB-43 (◇), and C_{18}-PEO-VB-35 (▽) in water with [M] = 45 mmol/L and [AVA] = 0.45 mmol/L. Solid symbols refer to the corresponding polymerization in benzene with [M] = 45 mmol/L and [AIBN] = 2.25 mmol/L.

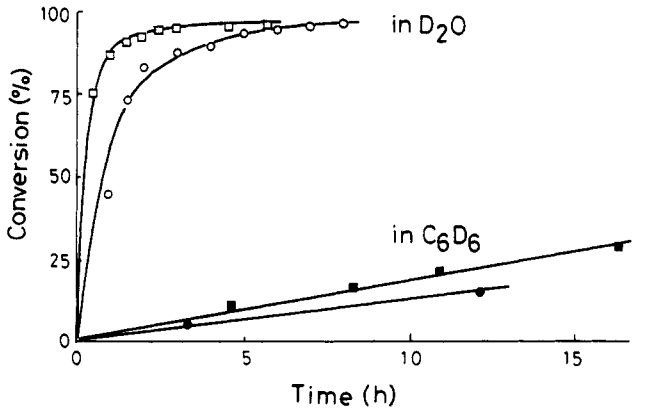

Figure 9. Conversion vs time plots for polymerization of C_1-PEO-MA-25 (□) and C_1-PEO-VB-25 (○) in water with [M] = 45 mmol/L and [AVA] = 0.45 mmol/L. Solid symbols refer to the corresponding polymerization in benzene with [M] = 45 mmol/L and [AIBN] = 2.25 mmol/L.

order as follows: R = C_{18} > C_8 > C_1 > C_4 > tC_4 and n = 17–25 > 45 > 60. As to the effect of n lower than 17, the model monomer, C_1-PEO-VB-4, is insoluble in water, but its polymerization appears to be much slower than C_1-PEO-VB-17, considering the results in benzene in Figure 6 together with those in water for R-PEO-MA-n in Figure 3. Therefore, the polymerizability of C_1-PEO-VB-n has its maximum around n = 10–25. A similar trend appears to be true with the other macromonomers, since the micelle formation will be unfavored with either too high or too low chain lengths of PEO. In this manner, the results observed in water reflect the effects of R and n on the formation of the micelle, the structure of which will in turn affect k_p and/or k_t, as will be discussed later.

The α-terminal directly determines the chemical reactivity of the macromonomer. Figure 9 as well as Figures 3–5 shows the higher rate of polymerization of the methacrylates than that of the corresponding p-vinylbenzyl ethers, both in benzene and in water, just as expected for the conventional monomers such as methyl methacrylate vs styrene.[14]

Molecular weights of some of the poly(macromonomer)s obtained were determined by means of a laser light scattering measurement in benzene with the results given in Table II, together with those estimated by GPC. First, it is important to note that the weight-average degree of polymerization, DP_w, was unusually high, just as observed for R_p, as compared to that expected for the conventional

Table II
Molecular Weights of Poly(macromonomer)s[a]

macromonomer	polymn solvent	LS[b] $10^{-6}M_w$	LS[b] DP_w	GPC[c] $10^{-6}M_w$	GPC[c] M_w/M_n
C_1-PEO-VB-25	water	10.0	8000	0.218	1.21
C_1-PEO-VB-45	water	6.4	3000	0.194	1.18
C_4-PEO-VB-39	water	3.0	1570	0.207	1.15
tC_4-PEO-VB-32	water	2.4	1500	0.146	1.25
C_1-PEO-VB-45	benzene	1.9	880	0.082	1.33

[a] Polymerization condition: [M] = 45 mmol/L, [I] = 0.45 mmol/L, at 60 °C for 24 h in water and 96 h in benzene. [b] Light scattering. [c] Gel permeation chromatography calibrated with linear PEO standard samples.

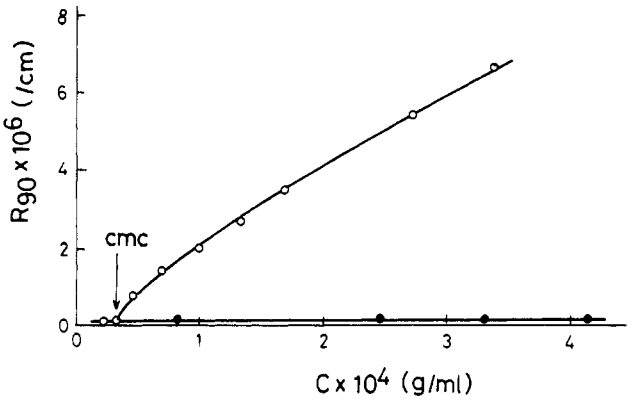

Figure 10. Rayleigh ratio at 90° (R_{90}) vs concentration for C_{18}-PEO-Bz-35 in water (○) and in benzene (●).

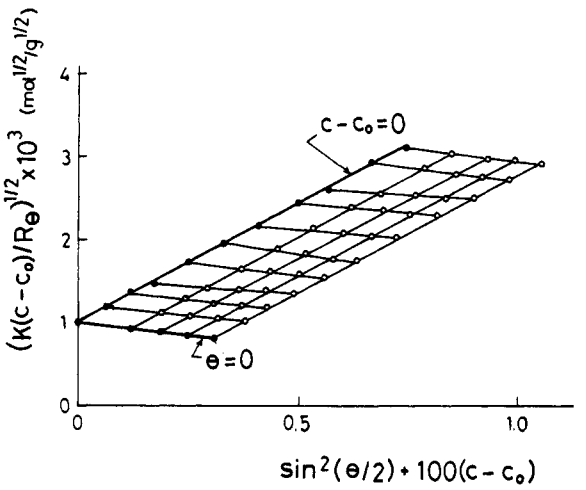

Figure 11. Modified Zimm–Berry plots for C_1-PEO-Bz-45 in water.

monomer under the same condition,[19] supporting the idea of the decrease in the diffusion-controlled bimolecular termination constant (k_t) and/or the increase in the propagation rate constant (k_p). Second, the effects of the ω-alkyl groups and the PEO chain lengths on the molecular weights just paralleled those on the polymerization rate. Third, the estimation by GPC of the molecular weights of these highly branched polymers cannot be justified so long as the conventional calibration is made with the linear polymers, as already pointed out for polystyrene macromonomers.[10] In fact, the viscosity measurements in benzene of the poly(macromonomers)s from C_1-PEO-VB-n have revealed that they have a very compact conformation, even to be approximated as a rigid sphere for n = 103,[20] so that GPC may severely underestimate their molecular weights.

Micelle Formation of Macromonomer Models in Water. The light scattering method[21] was applied to the nonpolymerizable models for the macromonomers in order

Table III
Micelle Formation of Macromonomer Models in Water at 25 °C[a]

macromonomer model	cmc, $\times 10^{-5}$ mol/L	M_m	m	$\langle s^2\rangle^{1/2}$, m	V_m, m^3	m/V_m, m^{-3}
C_1-PEO-Bz-25	3.3	2.1×10^6	1.8×10^3	1.7×10^{-7}	4.5×10^{-20}	4.0×10^{22}
C_1-PEO-Bz-45	3.0	1.1×10^6	5.2×10^2	1.7×10^{-7}	4.5×10^{-20}	1.2×10^{22}
C_4-PEO-Bz-39	5.8	3.4×10^4	1.9×10	7.6×10^{-8}	3.9×10^{-21}	4.9×10^{21}
tC_4-PEO-Bz-32	7.0	3.0×10^4	1.9×10	1.3×10^{-7}	2.1×10^{-20}	9.0×10^{20}
C_8-PEO-Bz-43	1.8	1.0×10^5	4.7×10	6.1×10^{-8}	2.0×10^{-21}	2.3×10^{22}
C_{18}-PEO-Bz-35	1.8	1.3×10^5	6.8×10	1.2×10^{-8}	1.4×10^{-23}	4.9×10^{24}
C_1-PEO-IB-25	7.1	2.3×10^4	1.9×10	2.5×10^{-8}	1.4×10^{-22}	1.4×10^{23}

[a] Subscript figures in the first decimal place indicate uncertainty of ±0.1 to ±0.3 in determining cmc, M_m, and $\langle s^2\rangle^{1/2}$.

to confirm their micelle formation in water and to estimate the cmc, the micellar molecular weight (M_m), and the root-mean-square radius of gyration ($\langle s^2\rangle^{1/2}$). Typically, Figure 10 clearly proves the micelle formation in water but not in benzene. In water, the scattering intensity or the Rayleigh ratio at 90° (R_{90}) increased with the concentration above that to be identified as cmc, while in benzene negligible scattering was observed, indicating the molecular dissolution of the same polymer. A modified Zimm–Berry plot[22] was constructed for the aqueous solution according to the equation

$$\left(\frac{K(c-c_0)}{R_\theta}\right)^{1/2} = \left(\frac{1}{M_m}\right)^{1/2}\left[1 + \frac{1}{6}\left(\frac{4\pi n_0}{\lambda_0}\right)^2 \langle s^2\rangle \sin^2\left(\frac{\theta}{2}\right) + A_2 M_m (c-c_0) + \ldots\right] \quad (5)$$

where

$$K = \frac{4\pi^2 n_0^2}{N\lambda_0^4}\left(\frac{dn}{dc}\right)^2 \quad (6)$$

with M_m the weight-average micellar weight, c the concentration, c_0 the cmc, A_2 the second virial coefficient, n_0 the refractive index of the solvent, dn/dc the refractive index increment of the solution, λ_0 the wavelength of the incident light, θ the scattering angle of observation, and N Avogadro's number. The concentration term, $c - c_0$, in place of c in the conventional treatment comes from the fact that the macromonomer model here shows no Rayleigh ratio below cmc, indicating that we are observing the scattering only from the micelles. Figure 11 shows an example of the modified Zimm–Berry plot. The estimated values of cmc, M_m, and $\langle s^2\rangle^{1/2}$ are summarized in Table III, together with the average number of aggregated monomers in each micelle, $m = M_m/M$ where M is the molecular weight of the macromonomer model, the average volume of the micelle, $V_m = 4\pi(5\langle s^2\rangle/3)^{3/2}/3$, assuming a sphere, and their ratio, m/V_m. Although the measurements were made at 25 °C,[23] with the nonpolymerizable models for the macromonomers, they should give useful insight for the micellar polymerization.

Among the parameters obtained, the ratio m/V_m appears to parallel closely with the polymerizability of the corresponding macromonomers. Since m/V_m means the average number of the molecules per unit volume of the micelle, it can be a measure of relative density of the molecules in the micelle, corresponding to that of the double bonds and/or of ω-alkyl groups of the macromonomers. Considering the constitution of the macromonomers (1 and 2) and their models (3 and 4), ω-alkyl groups except for methyl (C_1) and the α-polymerizing and their nonpolymerizing model groups are clearly hydrophobic so that they will be sure to construct the core of the micelle, while the hydrophilic PEO chains will coil around the core to make the shell. Therefore, it is reasonable to speculate the micelle structure of the macromonomers as

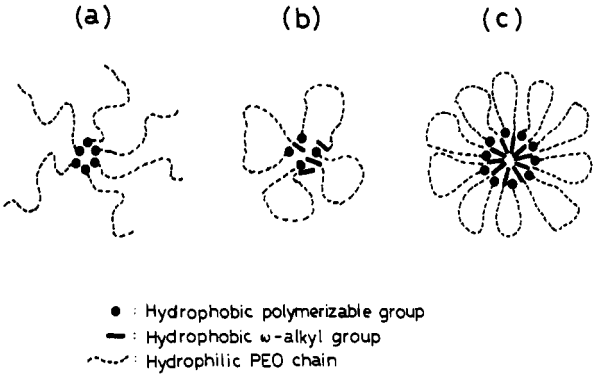

Figure 12. Schematic models of micelles of macromonomers with ω-alkyl groups: (a) C_1; (b) C_4, tC_4, and possibly C_8; (c) C_{18}.

given schematically in Figure 12.[24] Thus, C_1-PEO-VB or -MA, composed of the hydrophilic C_1-PEO segment and the hydrophobic VB or MA, will organize into a simple micelle as in (a), where the PEO chains will extend fully to allow a relatively compact arrangement of the hydrophobic α-terminals. On the other hand, the other macromonomers carrying hydrophobic groups at both ends of the hydrophilic PEO chains will organize into a micelle of smaller size because the PEO chains will be forced to assume looplike conformations as in the models (b) for R = C_4 or tC_4 and (c) for R = C_{18}. R = C_8 may stand intermediate between (b) and (c). Model (c) was presented as such because of the highly hydrophobic nature of the long alkyl groups, which will align themselves very compactly in the core with the other, less hydrophobic *p*-vinylbenzyl groups residing at the interphase to the surrounding hydrophilic shell composed of PEO chains.

These models, even if only schematic,[24] appear reasonable to account for the observed parallel trends in the polymerizability (R_p) and the molecular packing density in the micelle (m/V_m). Among the macromonomers investigated, C_{18}-PEO-VB polymerized the most rapidly, probably as a result of the most closed packing or orientation of the double bonds as in the model (c). C_1-PEO-VB polymerized moderately rapidly with the double bonds concentrated in the micelle core as in the model (a). It is reasonable that the moderately short PEO chain is more favorable for organization into the micelle and therefore also for polymerization as observed, because too long PEO will make the macromonomer too hydrophilic for organization of the α-terminal double bonds. The macromonomers with ω-alkyl groups of C_4, tC_4, or probably also C_8 polymerized most slowly probably because of loose packing of their double bonds together with the ω-alkyl groups as in the model (b).

In any case, the high polymerizability of these amphiphilic PEO macromonomers in water appears to be closely related to their organization into the micelle. This organization will clearly favor the propagation reaction (increase in k_p) and hinder the bimolecular termination (decrease in k_t).[25] Which factor is determining can be

answered with difficulty at present. It appears reasonable, however, to say that both factors are responsible for the observed effects of the ω-alkyl groups and the PEO chain lengths on the micellar polymerization, since they are not very significant in benzene in which k_t must be clearly a determining factor in changing the polymerizability.

Finally, it will be interesting to note that the degree of polymerization of the poly(macromonomer) obtained in Table II is 1 or more orders of magnitude higher than the degree of aggregation (m) in the micelle of the corresponding macromonomer model in Table III. This result suggests that the micellar polymerization involves the intermicellar propagation and/or termination or the reorganization of the micelle during polymerization. However, the light scattering measurements were made at 25 °C with the macromonomer models without double bonds and at concentrations more dilute as compared to those in polymerization. Micelles of much larger size may grow at higher temperature and concentration.[23,26]

Conclusion

Amphiphilic PEO macromonomers were found to polymerize in water with an unusually high rate that has not been observed for a solution polymerization of a conventional monomer or macromonomer. The effects of the ω-alkyl groups and the PEO chain lengths on their polymerizability, coupled with the laser light scattering study of their nonpolymerizable models, revealed the organization of these macromonomers into the micelles as the most important factor. The very rapid organized polymerization will be promising for a variety of potential applications based on the fixation of the amphiphilic (hydrophobic–hydrophilic) microdomains.

Acknowledgment. This work was supported in part by a Grant-in-Aid (No. 01470111) for General Scientific Research from the Ministry of Education, Science and Culture, Japan. We greatly appreciate Prof. T. Kato and Prof. A. Takahashi for their use of the refractometer, RF-600, and the Takemoto Oil & Fat Co., Ltd., for monostearyl ether of poly(ethylene glycol).

References and Notes

(1) (a) Yamashita, Y., Ed. *Makuromonoma no Kagaku to Kogyo (Chemistry and Industry of Macromonomers)*; IPC: Tokyo, 1989. (b) Rempp, P. F.; Franta, E. *Adv. Polym. Sci.* **1984**, *58*, 1.
(2) Tsukahara, Y.; Tanaka, M.; Yamashita, Y. *Polym. J.* **1987**, *19*, 1121.
(3) Gnanou, Y.; Lutz, P. *Makromol. Chem.* **1989**, *190*, 577.
(4) (a) Ito, K.; Tsuchida, H.; Kitano, T.; Yamada, E.; Matsumoto, T. *Polym. J.* **1985**, *17*, 827. (b) Ito, K.; Tsuchida, T.; Kitano, T. *Polym. Bull.* **1986**, *15*, 425. (c) Ito, K.; Yokoyama, S.; Arakawa, F.; Yukawa, Y.; Iwashita, N.; Yamasaki, Y. *Polym. Bull.* **1986**, *16*, 337. (d) Ito, K.; Arakawa, F.; Tanaka, H.; Hashimura, K.; Itsuno, S. *Rep. Asahi Glass Found. Ind. Technol.* **1989**, *54*, 105.
(5) (a) Kennedy, J. P.; Hiza, M. *J. Polym. Sci., Polym. Chem. Ed.* **1983**, *21*, 1033. (b) Kennedy, J. P.; Lo, C. Y. *Polym. Bull.* **1985**, *13*, 343.
(6) (a) Cameron, G. G.; Chisholm, M. S. *Polymer* **1985**, *26*, 437. (b) Cameron, G. G.; Chisholm, M. S. *Polymer* **1986**, *27*, 437. (c) Cameron, G. G.; Chisholm, M. S. *Polymer* **1986**, *27*, 1420.
(7) Tsukahara, Y.; Hayashi, N.; Jiang, X.-L.; Yamashita, Y. *Polym. J.* **1989**, *21*, 377.
(8) (a) Percec, V.; Wang, J. H. *J. Polym. Sci.: Part A: Polym. Chem.* **1990**, *28*, 1059. (b) Percec, V.; Eppl, U.; Wang, J. H.; Schneider, H. A. *Polym. Bull.* **1990**, *23*, 19.
(9) Ito, K.; Yokoyama, S.; Arakawa, F. *Polym. Bull.* **1986**, *16*, 345.
(10) Tsukahara, Y.; Mizuno, K.; Segawa, A.; Yamashita, Y. *Macromolecules* **1989**, *22*, 1546.
(11) Tsukahara, Y.; Tsutsumi, K.; Yamashita, Y.; Shimada, S. *Macromolecules* **1989**, *22*, 2869.
(12) Hatada, K.; Kitayama, T.; Masuda, E. *Makromol. Chem., Rapid Commun.* **1990**, *11*, 101.
(13) Presented in parts in the meetings with the preprints as follows. (a) Ito, K.; Tanaka, K.; Tanaka, H. *IUPAC 32nd Int. Symp. Macromol. (Kyoto, Jpn.), Prepr.* **1988**, 222. (b) Imai, G.; Toyomasu, S.; Ito, K.; Tanaka, K. *Polym. Prepr., Jpn.* **1988**, *37*, 1421. (c) Tanaka, H.; Hashimura, K.; Ito, K.; Tanaka, K. *Polym. Prepr., Jpn.* **1988**, *37*, 1424. (d) Tanaka, H.; Imai, G.; Kawaguchi, S.; Itsuno, S.; Ito, K. *Polym. Prepr., Jpn.* **1989**, *38*, 1317.
(14) Odian, G. *Principles of Polymerization*, 2nd ed.; Wiley: New York, 1981.
(15) The decomposition rates were followed by means of ^{1}H NMR by the disappearance of the peaks of the methyl protons of the initiators in reference to those of the internal standards, DSS in D_2O and HMDS in C_6D_6. The first-order plots gave the decomposition rate constants as follows: $k_d = 6.0 \times 10^{-6}$ s^{-1} and 8.3×10^{-6} s^{-1} for AVA in D_2O and AIBN in C_6D_6, respectively, in good accord with the literature data for AVA sodium salt and AIBN. (a) Blakley, D. C.; Haynes, A. C. *J. Chem. Soc., Faraday Trans. 1* **1979**, *75*, 935. (b) Brandrup, J., Immergut, E. H., Ed. In *Polymer Handbook*, 3rd ed.; Wiley: New York, 1989.
(16) North, A. M. *Kinetics of Free Radical Polymerization*; Pergamon: London, 1966.
(17) The viscosity of the solution of tC_4-PEO-Bz-24, M_n 1100, was measured in benzene at 25.0 °C with an Ubbelohde-type viscometer. The relative viscosity, η_{rel}, was found to depend on the concentration, [M], ranging from 13 to 161 mmol/L, according to the usual expression; $\eta_{rel} = 1 + 0.0405[M] + 0.0114 \times 10^{-2}[M]^2$.
(18) (a) Yeoh, K. W.; Chew, C. H.; Gan, L. M.; Koh, L. L. *Polym. Bull.* **1989**, *22*, 123. (b) Yeoh, K. W.; Chew, C. H.; Gan, L. M.; Koh, L. L.; Teo, H. H. *J. Macromol. Sci., Chem.* **1989**, *A26*, 663.
(19) By assuming a recombination termination with no transfer, $f = 1$ with k_d as determined for AIBN (ref 15), and the literature values of k_p and k_t (ref 14), the rate of polymerization, R_p as in eq 4, and the number-average degree of polymerization, $DP_n = 2k_p[M]/(2k_tk_df[I])^{1/2}$, were calculated to be as small as 8×10^{-8} mol L^{-1} s^{-1}, and 22, respectively, for styrene at [M] = 45 mmol/L and [I] = 0.45 mmol/L.
(20) (a) Tomi, Y.; Imai, G.; Ito, K. *Polym. Prepr. Jpn.* **1989**, *38*, 1657. (b) Tomi, Y.; Imai, G.; Kawaguchi, S.; Ito, K. *Polym. Prepr. Jpn.* **1990**, *39*, 166.
(21) Imae, T.; Ikeda, S. *J. Phys. Chem.* **1986**, *90*, 5216.
(22) Berry, G. C. *J. Chem. Phys.* **1966**, *44*, 4550.
(23) Cmc of C_{18}-PEO-Bz-35 was determined also at 30 and 40 °C to be 1.6 and 0.95×10^{-5} mol/L, respectively, indicating together with the value at 25 °C in Table III that the micelle formation is entropically favored with increasing temperature, in accord with the conventional nonionic surfactants: (a) Meguro, K.; Ueno, M.; Esumi, K. In *Nonionic Surfactants*; Schick, M. J., Ed.; Marcel Dekker: New York, 1987; p 109. (b) Corkill, J. M.; Goodman, J. F.; Tate, J. R. *Trans. Faraday Soc.* **1964**, *60*, 996.
(24) The models illustrated should be taken only as schematic just for representing relative shapes and orders in organization into the micelle. The radius of gyration $\langle s^2 \rangle^{1/2}$ determined in Table III, particularly for C_1-PEO-Bz, is much larger than that expected for the fully extended conformation of the PEO chains (ca. 90 Å or 0.09×10^{-7} m for the end-to-end distance of PEO with $n = 25$). Therefore, the micelle should be actually of a much more loosely organized structure, even including their higher order aggregations.
(25) It is to be noted that a simple accumulation of the double bonds or an increased local monomer concentration will only explain the enhanced R_p but cannot explain by itself the enhanced rate of *conversion* as observed. The linear dependence of R_p on [M], as in eq 3 or 4, means the independence of the conversion on [M],[14] because the conversion, which corresponds to $-d[M]/[M]$ or its integrated form, already includes normalization in term of the monomer concentration. Therefore, by virtue of eq 4, the enhanced conversion requires either an increase in k_p or a decrease in k_t, under a reasonable assumption of constant k_d and f.
(26) Funahashi, N.; Hada, S.; Neya, S. *Bull. Chem. Soc. Jpn.* **1989**, *62*, 2485.